

Transport properties of epitaxial graphene grown on SiC substrate

SELMAN AĞIZAÇMAK^a, REMZIYE TÜLEK^a, SIBEL GÖKDEN^{a,*}, ALI TEKE^a, ENGIN ARSLAN^b, AYŞE MELİS AYGAR^c, EKMEL ÖZBAY^b

^aDepartment of Physics, Faculty of Science and Letter, Balıkesir University, Çağış Kampüsü, 10145 Balıkesir, Turkey

^bNanotechnology Research Center-NANOTAM, Department of Physics, Department of Electrical and Electronics Engineering, Bilkent University, 06800 Ankara, Turkey

^cDepartment of Electrical and Computer Engineering, McGill University, Montréal, Quebec H3A2A7, Canada

In this study, the Hall effect measurement of graphene on SiC substrate was carried out as a function of temperature (12-300 K). Hall data were first analyzed to extract the temperature dependent mobilities and carrier densities of the bulk (3D) and two dimensional (2D) channels using a Simple Parallel Conduction Extraction Method (SPCEM) successfully. High carrier mobility $2.296 \text{ cm}^2/\text{V}\cdot\text{s}$ from the graphene layer and low carrier mobility $813 \text{ cm}^2/\text{V}\cdot\text{s}$ from the SiC were obtained at room temperature. By using SPCEM extracted data, 3D and 2D scattering mechanisms were analyzed and the dominant scattering mechanisms in low and high temperature regimes were determined. It was found that the transport was mainly determined by scattering processes in 2D graphene.

(Received July 12, 2016; accepted April 6, 2017)

Keywords: 2D graphene, Scattering, SPCEM analysis, Hall effect, Transport

1. Introduction

Graphene based systems have attracted considerable attention after Novoselov et al. [1-4]. Graphene is a two dimensional form of atoms in a honeycomb lattice [1] and stable chemically and mechanically due to its tightly packed carbon atoms and sp^2 orbital hybridization. It combines high electron mobility with atomic thickness, and it promises wide spread applications [5-9]. Although graphene displays remarkable mobility with reported values in excess of $200.000 \text{ cm}^2\cdot\text{V}^{-1}\cdot\text{s}^{-1}$ for free standing wafer [2], it significantly reduces for wafers grown on different substrate. The mobility of monolayer graphene grown on SiC was reported in the range of $50\text{-}45.000 \text{ cm}^2\cdot\text{V}^{-1}\cdot\text{s}^{-1}$ [10-12]. Similarly, the graphene layer grown or transferred on different substrate (SiO_2 , Ni, Ru, Ir, Cu) have shown lower or higher mobilities. Therefore, it is important to investigate the mobility limiting mechanism in 2D graphene grown on substrate. In 2D semiconductor systems, the overall transport may be governed by charge carriers present in both 2D channel and bulk region of materials that have different electrical transport properties. To extract the transport parameters of a 2D channel from that of bulk, several extraction techniques were proposed [13-18] in the literature. Among those, the Simple Parallel Conduction Extraction Method (SPCEM), which was proposed by Lisesivdin et al. [19], is the simplest and most effective approach. The extraction of the mobilities and carrier densities of the multiple channels present in various material systems, such as AlGaIn/GaN [19, 20], AlInN/GaN heterostructures [21], and graphene/SiC

[22,23], was performed successfully using this simple approach.

In this study, SPCEM analysis was performed on Hall effect data taken at a low magnetic field of 0.5 T. This allowed for eliminating the possible effects of oscillations in resistivity at low temperatures and high magnetic fields. The measured temperature dependent Hall mobilities and carrier densities of 2D graphene and bulk SiC substrate were first extracted using SPCEM and then, the mobilities of carriers in both channels were analyzed by including the main scattering mechanisms that govern the transport properties in the temperature range of 12- 300K.

2. Experimental details

Hall measurements were taken on epitaxial graphene grown on $(10\times 10) \text{ mm}^2$ nominally on axis Si-face chemomechanically polished 4H-SiC (0001) substrate. Single layer graphene formation was verified with standard Raman measurements with an excitation source of 532 nm (2.33 eV) He-Ne laser was used. The samples were exposed to a mixture of silane and hydrogen (0.006% silane in hydrogen) for 10 min at 1400°C . The growth of graphene was performed in vacuum ($5\text{-}9 \times 10^{-6} \text{ mbar}$) for 1 hour and then cooled to 500°C . The growth cell was then filled with hydrogen to a pressure of 500 mbar and a one hour intercalation process was completed at 700°C . Hall bar geometry was transferred to graphene wafer using optical lithography with a suitable photo mask fabricated with electron beam lithography for Hall effect measurements. Ohmic contacts were fabricated with the

reverse lithography technique. After development, lift-off and etching processes the active graphene region with 500 μm by 1100 μm size was obtained. Interconnect metal lithography was performed by using 30 nm/220 nm Ti/Au metal pair. The details of the fabrication processes were given in reference 22. Hall effect measurements were made as a function of temperature between 12 and 300 K by using a cooling system. A constant low magnetic field ($B=0.5$ T) was applied to the sample perpendicular to the current plane. A constant current source (Keithley 2400) and a nanovoltmeter (Keithley 2182A) were used in the measurements.

3. Theory

In the application of SPCEM analysis, some assumptions are made [19]. (i) Only the carriers in the 2D graphene layer and 3D SiC substrate are considered as the two main contributions to total conductivity. (ii) At low temperatures, bulk carriers are assumed to be frozen. Therefore, the Hall carrier density at the lowest temperature (it was obtained by finding the interception of the best fitting using suitable polynomial order) is expected to be only related to the temperature independent 2D carriers. (iii) Because of thermal activation of bulk carriers, the temperature dependence of the measured carrier density would be associated with bulk carriers only. (iv) The density of bulk carriers and 2D carriers are approximately in the same order at high temperatures. The carrier density and the mobility of 2D and bulk carriers were calculated separately with these assumptions.

In the SPCEM calculation, the mobility of 2D carrier (μ_{2D}), and bulk carrier (μ_{Bulk}) were calculated by [19],

$$\mu_{2D} = \mu_H \sqrt{\frac{n_H}{n_{2D}}}, \quad (1)$$

$$\mu_{Bulk} = \mu_H \frac{n_H - n_{2D}}{n_H} = \mu_H \frac{n_{Bulk}}{n_H} \quad (2)$$

where μ_H is the experimental Hall mobility at a single magnetic field. At the lowest temperature available, $n_{2D} = n_H$ is taken and this is used for all temperatures because of temperature independent 2D carrier densities. For the bulk carrier density $n_{Bulk} = n_H - n_{2D}$ is used.

Scattering mechanisms used for 2D carriers:

In the investigation of total limited mobility in graphene on SiC (μ_{2D}), longitudinal acoustic (LA) phonon scattering limited mobility (μ_{LA}) [24,25], remote interfacial phonon (RIP) scattering limited mobility (μ_{RIP}) [26], and temperature independent scattering mobility term (μ_0) [23] are used in Matthiessen's rule as [19],

$$\frac{1}{\mu_{2D}} = \frac{1}{\mu_{LA}} + \frac{1}{\mu_{RIP}} + \frac{1}{\mu_0} \quad (3)$$

The parameters of graphene that are used in 2D scattering analysis are given in Table 1 [23-25].

Table 1. Parameters of graphene used in 2D scattering calculations [23-25]

Parameter	Value
D_A (eV)	18
ρ_s ($\times 10^{-7}$ kg/m ²)	7.6
v_s ($\times 10^4$ m/s)	2.1
v_f ($\times 10^6$ m/s)	1

LA phonon scattering: LA phonon scattering in graphene can be given as [24]

$$\mu_{LA} = \frac{4e\hbar\rho_s v_s^2 v_f^2}{n_{2D} \pi D_A^2 k_B T} \quad (4)$$

where, D_A , ρ_s , v_s , v_f and k_B are deformation potential, 2D mass density of graphene, LA phonon velocity, the Fermi velocity of graphene and the Boltzmann constant, respectively.

RIP phonon scattering: Optical phonons at the surface and subsurface of the graphene layer cause the RIP scattering in graphene [26],

$$\mu_{RIP} = \frac{1}{n_{2D} e} \left[\sum_i \left(\frac{C_i}{\exp(E_i/k_B T) - 1} \right) \right]^{-1} \quad (5)$$

where, C_i and E_i are fitting parameters for coupling strength and phonon energy, respectively.

Temperature independent scattering terms: The temperature independent scattering mobility (μ_0), which includes Coulomb scattering (μ_C) and short range scattering (μ_{SR}) terms as [21]

$$\frac{1}{\mu_0} = \frac{1}{\mu_C} + \frac{1}{\mu_{SR}} \quad (6)$$

Short range scattering is $\mu_{SR} = A/n_{2D}$ [27], where A is constant. From the assumption of SPCEM, 2D carrier density is temperature independent and, therefore, short range scattering is constant. Moreover, μ_C is constant; it is possible to calculate the contribution of each scattering term to μ_0 . Therefore, instead of μ_C and μ_{SR} , μ_0 is calculated.

Scattering mechanisms used for bulk carriers: Acoustic phonon scattering is limited bulk mobility of SiC [27]. The parameters of SiC that are used in 3D scattering analysis are given in Table 2 [29-31].

Table 2. Parameters of SiC used in bulk scattering calculations [29-31]

Parameter	Value
m^* (xm_0)	0.29
ϵ_s ($x \epsilon_0$)	10.03
ϵ_0 ($x10^{-12}$ F/m)	8.85
$\hbar\omega_{po}$ (meV)	197
c_{LA} ($x10^{11}$ N/m ²)	5.07
E_D (eV)	18
k ($x10^8$ m ⁻¹)	8.92

Acoustic phonon scattering: Acoustic phonon scattering includes deformation potential (DP) and piezoelectric (PE) polarization fields. Deformation potential scattering limited mobility is given by [28],

$$\mu_{DP} = \frac{\pi \hbar^5 c_{LA}^2}{E_D^2 k_B T m^{*2} k} \left[1 - \frac{q_{s3D}^2}{k^2} + \frac{q_{s3D}^4}{8k^2} \left(3 \ln \left[1 + \left(\frac{2k}{q_{s3D}} \right)^2 \right] - \frac{1}{1 + (q_{s3D}/2k)^2} \right) \right]^{-1} \quad (7)$$

Where E_D is the deformation potential constant, c_{LA} is the elastic constant, k is the electron wave vector, m^* is the effective mass and q_{s3D} is the reciprocal screening length in 3D,

$$q_{s3D}^2 = -\frac{e^2}{\epsilon_s} \int \frac{df(E)}{dE} N(E) d(E) \quad (8)$$

where $f(E)$ is the Fermi Dirac Function and $N(E)$ is the density of states function. The piezoelectric scattering limited mobility is given as [28],

$$\mu_{PE} = \frac{2\pi \epsilon_s \hbar^5 k}{K^2 e k_B T m^{*2}} \left[1 - \frac{q_{s3D}^2}{k^2} + \frac{q_{s3D}^4}{8k^2} \left(3 \ln \left[1 + \left(\frac{2k}{q_{s3D}} \right)^2 \right] - \frac{1}{1 + (q_{s3D}/2k)^2} \right) \right]^{-1} \quad (9)$$

Where K is the electromechanical coupling coefficient and ϵ_s is the static dielectric constant. The total acoustic phonon limited mobility is calculated with Matthiessens's rule,

$$\frac{1}{\mu_{AC}} = \frac{1}{\mu_{DP}} + \frac{1}{\mu_{PE}} \quad (10)$$

Polar optical phonon scattering: Polar optical phonon scattering, which is the dominant scattering mechanism at high temperature, limited mobility is given by [28],

$$\mu_{PO(Bulk)} = \frac{e^2 \tau_m}{m^*} e^{\hbar\omega_{PO}/k_B T} \quad (11)$$

where $\hbar\omega_{PO}$ is the polar optical phonon energy and τ_m is the momentum relaxation time.

Ionized impurity scattering: The mobility limited by ionized impurity scattering which is an elastic scattering process is given as [28]

$$\mu_{II} = \sqrt{\frac{128 (k_B T)^3}{m^* \pi^3}} \frac{(4\pi \epsilon_s)^2}{Z^2 e^3 N_{imp} [\ln(1+\beta^2) - \frac{\beta^2}{1+\beta^2}]} \quad (12)$$

where, Z is the charge of ionized atom that is taken as unity, N_{imp} is the density of ionized impurities, and β is described as,

$$\beta = \frac{2m^*}{\hbar} \lambda_D \sqrt{\frac{2}{m^*} 3k_B T} \quad (13)$$

where λ_D is the 3D screening length and described as,

$$\lambda_D = \sqrt{\frac{k_B T \epsilon_s}{e^2 n_{Bulk}}} \quad (14)$$

4. Results and discussion

Fig. 1 shows the temperature dependence of Hall mobilities and the carrier density of the graphene/SiC in the temperature range between 12 and 300 K. Low temperature Hall mobility of 5000 cm²/V.s decreases to 1620 cm²/V.s at room temperature. On the other hand, the measured total carrier density which comprises both bulk and 2D types increases as the temperature increases. From the interception of fitting curve to the total carrier density axis, the sheet carrier density related only to the 2D grapheme layer is found to be 1.054×10¹¹ cm⁻². Because the 2D carrier density is expected to become temperature independent [19], the excess carriers can be attributed to the thermally activated bulk carriers in SiC.

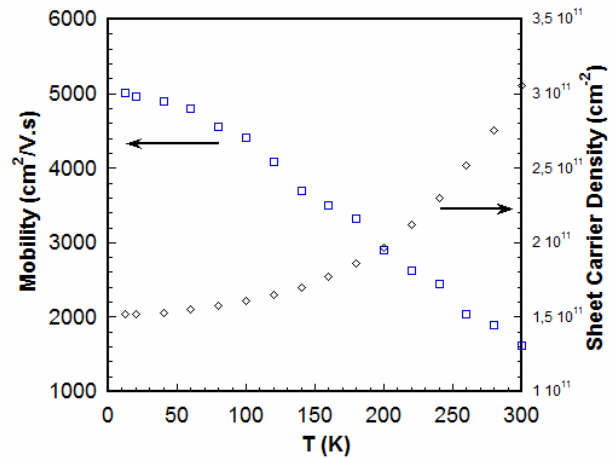


Fig. 1. Temperature dependent electron mobility and sheet carrier density values.

Mobility and sheet carrier density as a function of temperature that are extracted from SPCEM are shown in Fig. 2(a) and 2(b), respectively. From SPCEM, the mobility in 2D graphene layer and bulk SiC are calculated

to be $2296 \text{ cm}^2/\text{V.s}$ and $813 \text{ cm}^2/\text{V.s}$ at room temperature, respectively.

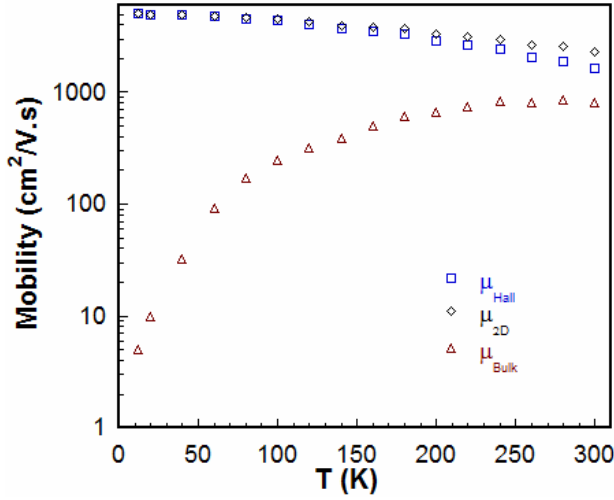


Fig. 2a. Mobilities of Hall measurement and SPCEM extracted 2D and bulk carriers

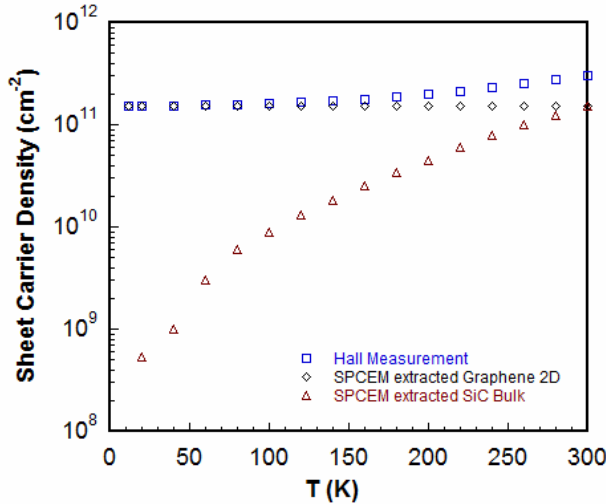


Fig. 2b. Sheet carrier densities of Hall measurement and SPCEM extracted 2D and bulk carriers

The extracted Hall mobility from SPCEM analysis along with the main scattering mechanisms related to the 2D graphene layer and 3D SiC substrate are shown in Fig. 3a and 3b, respectively. As seen in Fig. 3a, temperature independent mobility (μ_0) which includes Coulomb scattering and short range scattering, is the dominant scattering mechanisms at low temperature. At higher temperatures, the mobility is limited by combination of temperature independent scattering (μ_0), and Remote Interfacial Phonon scattering (μ_{RIP}). In Fig. 3b, the dependence of mobility on temperature clearly behave as a usual 3D character, where the ionized impurity scattering is dominant at low temperature, and as the temperature increases the scattering due to acoustic and optic phonons become effective in the determination of the total mobility

value. From the bulk scattering analysis, ionized impurity concentration and the momentum relaxation time for LO-phonons are determined as $5 \times 10^{22} \text{ m}^{-3}$ and $1.4 \times 10^{16} \text{ s}$, respectively.

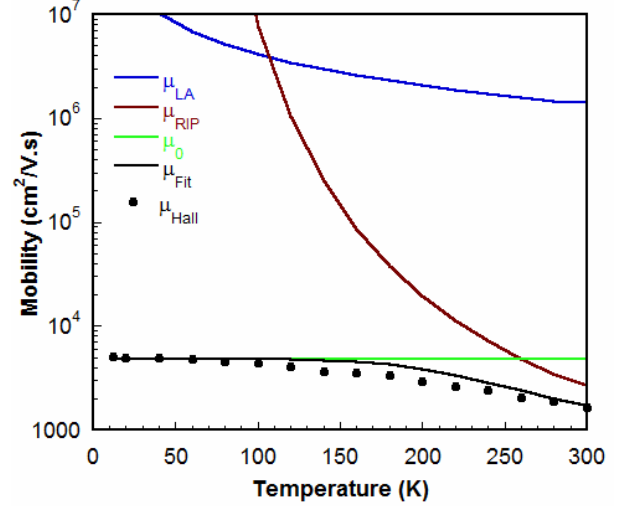


Fig. 3a. Scattering analysis of SPCEM extracted 2D (graphene)-carrier

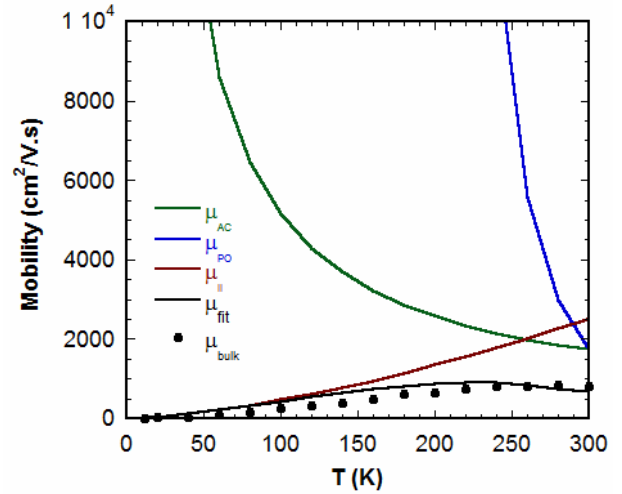


Fig. 3b. Scattering analysis of SPCEM extracted bulk (SiC)-carrier

5. Conclusions

Hall effect measurements of graphene on SiC substrate were carried out as a function of temperature (12-300 K) at low magnetic field (0.5T). By using Hall data temperature dependent mobilities and carrier densities of 2D carrier of graphene and bulk carrier of SiC substrate were calculated with SPCEM. From the analyzed high carrier mobility $2296 \text{ cm}^2/\text{V.s}$ from the graphene layer and low carrier mobility $813 \text{ cm}^2/\text{V.s}$ from the SiC were obtained at high temperature. By using SPCEM extracted carrier data, 3D and 2D scattering mechanisms were analyzed and dominant scattering mechanisms in low and high temperature regimes were determined. It was found

that the transport was determined by the combination of 2D from graphene and 3D from SiC scattering processes.

References

- [1] K. S. Novoselov, A. K. Geim, S. V. Morozov, D. Jiang, Y. Zhang, S. V. Dubonos, I. V. Grigorieva, A. A. Firsov, *Science* **306**, 666 (2004).
- [2] A. K. Geim, K. S. Novoselov, *Nature Materials* **6**, 183 (2007).
- [3] A. H. C. Neto, F. Guinea, N. M. R. Peres, K. S. Novoselov, A. K. Geim, *Rev. Modern Phys.* **81**(1), 109 (2009).
- [4] D. Wei, Y. Liu, Y. Wang, H. Zhang, L. Huang, G. Yu, *Nano Lett.* **9**(5), 1752 (2009).
- [5] V. V. Cheianov, V. Falko, B. L. Altshuler, *Science* **315**(5816), 1252 (2007).
- [6] X. L. Li, X. R. Wang, L. Zhang, S. W. Lee, H. J. Dai, *Science* **319**, 1229 (2008).
- [7] D. A. Areshkin, C. T. White, *Nano Lett.* **7**(11), 3253 (2007).
- [8] S. V. Morozov, K. Novoselov, M. Katsnelson, F. Schedin, D. Elias, J. Jaszczak, A. Geim, *Phys. Rev. Lett.* **100**(1), 016602 (2008).
- [9] J. H. Chen, C. Jang, S. Xiao, M. Ishigami, M. S. Fuhrer, *Nature Nanotec.* **3**, 206 (2008).
- [10] E. Pallecchi, F. Lafont, V. Cavaliere, F. Schopfer, D. Mailly, W. Poirier, A. Ouerghi, *Scientific Reports* (2014).
- [11] W. Norimatsu, M. Kusunoki, *Phys. Chem. Chem. Phy.* **16**(8), 3501 (2014).
- [12] S. Tanabe, Y. Sekine, H. Kageshima, M. Nagase, H. Hibino, *Phys. Rev. B* **84**(11), 115458 (2011).
- [13] M. J. Kane, N. Apsley, D. A. Anderson, L. L. Taylor, T. Kerr, *J. Phys. C: Solid State Phys.* **18**(29), 5629 (1985).
- [14] W. A. Beck, J. R. Anderson, *J. Appl. Phys.* **62**(2), 541 (1987).
- [15] J. R. Meyer, C. A. Hoffman, F. J. Bartoli, D. J. Arnold, S. Sivananthan, J. P. Faurie, *Semicond. Sci. Technol.* **8**(6S), 805 (1993).
- [16] S. P. Tobin, G. N. Pultz, E. E. Krueger, M. Kestigian, K. K. Wong, P. W. Norton, *J. Electron. Mater.* **22**(8), 907 (1993).
- [17] Z. Dziuba, J. Antoszewski, J. M. Dell, L. Faraone, P. Kozodoy, S. Keller, B. Keller, S. P. DenBaars, U. K. Mishra, *J. Appl. Phys.* **82**(6), 2996 (1997).
- [18] S. B. Lisesivdin, N. Balkan, E. Özbay, *Microelectronics J.* **40**(3), 413 (2009).
- [19] S. B. Lisesivdin, A. Yildiz, N. Balkan, M. Kasap, S. Özcelik, E. Özbay, *J. Appl. Phys.* **108**(1), 013712 (2010).
- [20] A. Yildiz, S. B. Lisesivdin, M. Kasap, S. Ozcelik, E. Ozbay, N. Balkan, *Appl. Phys. A* **98**(3), 557 (2010).
- [21] R. Tülek, E. Arslan, A. Bayraklı, S. Turhan, S. Gökden, Ö. Duygulu, A. A. Kaya, T. Fırat, A. Teke, E. Özbay, *Thin Solid Films* **551**, 146 (2014).
- [22] E. Arslan, S. Çakmakyapan, Ö. Kazar, S. Bütün, S. B. Lisesivdin, N. A. Cinel, G. Ertaş, S. Ardalı, J. Ul-Hassan, E. Janzen, E. Özbay, *Electron. Mater. Lett.* **10**, 387 (2014).
- [23] S. B. Lisesivdin, G. Atmaca, E. Arslan, S. Çakmakyapan, Ö. Kazar, S. Bütün, J. Ul-Hassan, E. Janzen, E. Özbay, *Physica E* **63**, 87 (2014).
- [24] J. H. Chen, C. Jang, S. Xiao, M. Ishigami, M. Fuhrer, *Nat. Nanotechnol.* **3**, 206 (2008).
- [25] W. Zhu, V. Perebeinos, M. Freitag, P. Avouris, *Phys. Rev. B* **80**(23), 235402 (2009).
- [26] S. Fratini, F. Guinea, *Phys. Rev. B* **77**(19), 195415 (2008).
- [27] C. Yu, J. Li, Q. B. Liu, S. B. Dun, Z. Z. He, X. W. Zhang, S. J. Cai, Z. H. Feng, *Appl. Phys. Lett.* **102**(1), 013107 (2013).
- [28] B. K. Ridley, B. E. Foutz, L. F. Eastman, *Phys. Rev. B* **61**(24), 16862 (1998).
- [29] D. Sun, Z. Wu, C. Divin, X. Li, C. Berger, W. A. de Heer, P. N. First, T. B. Norris, *Phys. Rev. Lett.* **101**, 157402 (2008).
- [30] L. Patrick, W. J. Choyke, *Phys. Rev. B* **2**(6), 2255 (1970).
- [31] N. T. Son, W. M. Chen, O. Kordina, A. O. Konstantinov, B. Monemar, E. Janzen, D. M. Hofman, D. Volm, M. Drechsler, B. K. Meyer, *Appl. Phys. Lett.* **66**(9), 1074 (1995).

*Corresponding author: sozalp@balikesir.edu.tr